

Simulation of the growth dynamics of amorphous and microcrystalline silicon

J. Bailat ^{*}, E. Vallat-Sauvain, A. Vallat, A. Shah

Institut de Microtechnique, Université de Neuchâtel, Breguet 2, CH-2000 Neuchâtel, Switzerland

Abstract

The qualitative description of the major microstructure characteristics of microcrystalline silicon is achieved through a three-dimensional discrete dynamical growth model. The model is based on three fundamental processes that determine surface morphology: (1) random deposition of particles, (2) local relaxation and (3) desorption. In this model, the incoming particle reaching the growing surface takes on a state variable representing a particular way of being incorporated into the material. The state variable is attributed according to a simple selection rule that is characteristic of the model. This model reproduces most of the features of the complex microstructure of microcrystalline silicon: transition from amorphous to crystalline phase, conical shape of the crystalline domains, crystalline fraction evolution with respect to the layer thickness and roughness evolution versus layer thickness.

1. Introduction

Hydrogenated microcrystalline silicon ($\mu\text{c-Si:H}$) prepared from a silane and hydrogen mixture by plasma-enhanced chemical vapor deposition (PECVD) is a promising material for large-area thin-film solar cells [1]. However, in order to improve the control of the deposition process, a better understanding of the material microstructure, the growth mechanisms and the growth dynamics is yet to be obtained.

The complex microstructure of $\mu\text{c-Si:H}$ material consists of conical nanocrystalline domains (thereafter called crystalline grains) growing with a conical shape of 15° [2], in a basic form, that is rather insensitive to experimental growth conditions. The grains are separated by amorphous material and in certain cases by voids or cracks.

Whereas microscopic growth mechanisms are still debated [3,4], experimental evidence of the role of desorption (e.g. preferential amorphous silicon etching)

and the absence of long-range diffusion of the adatoms on the surface are now accepted.

The growth dynamics of microcrystalline materials have been experimentally studied with real-time spectroscopic ellipsometry [5] and the evolution of surface morphology has been characterized by atomic force microscopy (AFM), on a series of sample of increasing thickness [6]. These studies revealed the occurrence of an amorphous to microcrystalline transition versus film thickness; this transition coincides with a sudden increase of surface roughness.

In this paper we propose an original approach to understanding the microstructure evolution, based on a simple discrete model. Discrete models have been successfully applied to the description of a variety of growth phenomena, from those involved in molecular beam epitaxy (MBE) to those occurring in the growth of bacterial colonies [7]. The model presented here is focused on capturing the essential mechanisms that lead to the microstructure evolution that is experimentally observed in $\mu\text{c-Si:H}$. It uses two simple selection rules:

- After deposition and local relaxation, the first selection rule applies to a discrete state variable associated with the particle: an incoming particle tends to be in the same state as its neighbors. This self-organization

^{*} Corresponding author. Tel.: +41-32 718 32 00; fax: +41-32 718 32 01.
E-mail address: julien.bailat@unine.ch (J. Bailat).

process is responsible for the growth of crystalline domains and their conical shape as experimentally observed;

- the second selection rule allows for deposited particle removal (desorption), corresponding thus, to the experimental observation that amorphous silicon is preferentially etched.

2. Simulation and experiment

2.1. Description of model used for simulation

A particle is released from a position randomly chosen above the surface. The particle follows a vertical trajectory in a cubic lattice until it reaches the growing surface whereupon it stops. The particle then moves to the lowest site within the first and second nearest neighbors where it sticks.

After this so-called relaxation process, the particle is given a state among n possible states (n is the first model parameter) with the following selection rule:

- The most represented state among the neighbors called thereafter the dominant state is evaluated. The neighborhood taken into account for this calculation extends over the 25 nearest neighbors, i.e. the nine neighbors below, the eight neighbors around and the eight neighbors above the selected site.
- If the number of particles in the dominant state is strictly higher than the crystalline threshold parameter t (the second model parameter), the particle's state is given the value of the dominant state, otherwise its state is randomly set to one of the n possible states. The crystalline threshold t is a model parameter comprised between 0 and 25 (25 being the maximum number of neighbors in this case).

The process of desorption (here, preferential etching of disordered material) is entered with a probability given by the third model parameter: the desorption process probability d . The selection rule for desorption is the following:

- The particle is immediately removed again, randomly, with a probability given by the ratio of the number of neighbors in a different state over the total number of neighbors. Thus, if all the neighbors are in a different state, the newly deposited particle will be removed.

After the selection rules have been applied, a new particle is deposited, until the set layer thickness is reached.

In this computer simulation, a state is represented by a color. A crystalline region is thus defined as a domain

of the cubic lattice filled with particles of the same color. In contrast with this, an amorphous region is a domain filled with randomly varying colors.

The simulations were carried out in $512 \times 512 \times 256$ network units for the rough substrate (Figs. 1 and 2) and in $256 \times 256 \times 256$ on the flat substrate (Fig. 3). Note that the particles impinging on the substrate cannot take the value of a state representing the substrate. Furthermore, the substrate sites are not counted as neighbors for the application of the selection rules.

2.2. Growth experiments and measurements

In this study a microcrystalline layer was deposited by PECVD on a rough substrate for comparison of the microstructure with the one generated by computer simulation. The approximately 400 nm thick i -layer was deposited at a silane gas phase concentration close to the a -Si:H/ μ c-Si:H transition. The underlying substrate material is a sodium-free AF-45 glass substrate coated with ZnO deposited by low pressure chemical vapor deposition, the latter being a rough transparent conductive oxide used for solar cells applications [8].

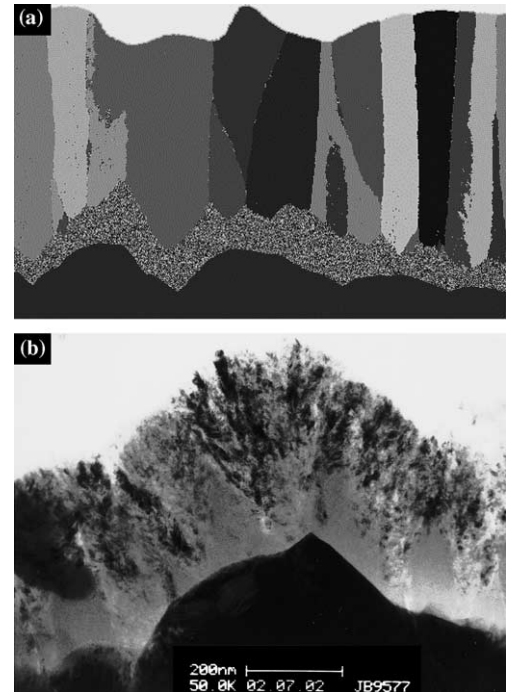


Fig. 1. (a) Cross-section through a 3D-simulated layer on a rough substrate. The model parameters are $n = 12$, $t = 6$, $d = 0.8$, layer thickness of 256 network units, substrate size of 512×512 network units. The uniform domains represent the microcrystalline grains and the dotted domain represents the amorphous phase. In this simulation the discretization of the AFM scan of the rough substrate yields a network unit size of about 2 nm. (b) Bright field TEM cross-section of a μ c-Si:H layer deposited by PECVD on a rough substrate. Amorphous silicon appears homogeneously grey, whereas the conical conglomerates of nanocrystallites show high contrast.

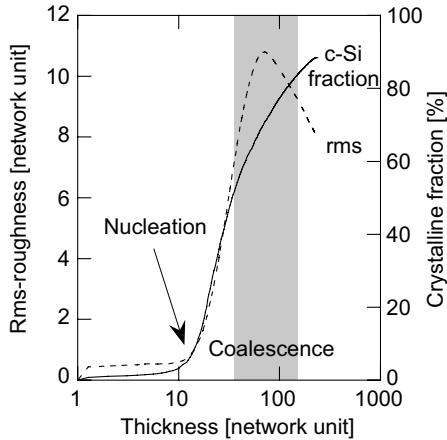


Fig. 2. Evolution of rms-roughness and crystalline fraction versus accumulated film thickness for a simulated layer on a flat substrate (same model parameters as in Fig. 1(a)). The roughness increases abruptly at nucleation, i.e. when crystalline fraction starts to increase, and reaches a maximum when the grains coalesce. The rms-roughness then decreases slightly as experimentally observed in [3].

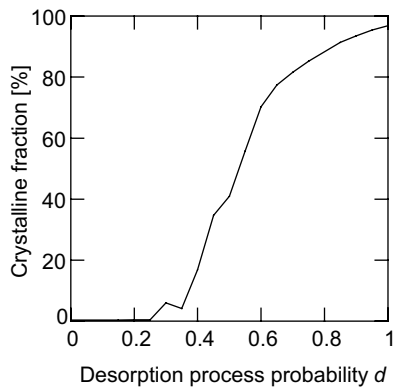


Fig. 3. Evolution of the crystalline fraction of simulated layers (256 network unit thick on a flat substrate of 256×256 network units) with respect to desorption process probability d . The other model parameters are $n = 12$ and $t = 6$. The simulated layer deposited with $d = 0$ is fully amorphous. When d rate parameter is increased the layer gets more and more crystalline to finally reach a crystalline fraction close to 100%. For each value of d , the crystalline fraction has been averaged on five simulated layers.

An AFM height scan (scan range of $1 \mu\text{m}$, 512×512 measurement points) of the substrate (here solar-grade LPCVD ZnO) has been used as a discrete height map for the computer simulations.

The samples were prepared as cross-sections for TEM examination with the help of the technique described in [9]. Transmission electron microscopy (TEM) observations were made in a Philips CM200 microscope operated at 200 kV. They allowed us to observe directly the microstructure of the layers, in particular: the morphology of the growing surface as well as that of the crystalline grains and of the distribution of the amorphous material within the layer.

3. Results

Simulated microstructure and TEM micrograph of a real layer on rough substrate are presented in Fig. 1. The model parameters chosen for this simulation were $n = 12$ states (i.e. colors), crystalline threshold $t = 6$ (remember that the number of neighbors in the same state for the incoming particle to take this state must be strictly higher than t and a desorption process probability $d = 0.8$). The simulated microstructure qualitatively shows the most important features of the comparison layer. Indeed, it exhibits a mixed-phase layer, the so-called ‘heterophase’ layer, where $\mu\text{c-Si:H}$ grains extend laterally to the detriment of the amorphous phase. The conical grains coalesce above the heterophase layer and from then onwards, the microstructure consists of microcrystalline columns that compete for lateral growth. The behavior of rms-roughness with respect to thickness evolution of the layer [5,6] is also well reproduced by the model (Fig. 2): once the nucleation occurs within the amorphous material, roughness increases as long as the coalescence threshold is not reached; thereafter, coalescence roughness decreases and finally stabilizes.

When the desorption process probability d is varied, one observes in Fig. 3 that the material structure changes from fully amorphous ($d = 0$) to crystalline ($d = 1$). If a higher value of d is assumed in the simulation, nucleation occurs at a lower height within the layer, as one indeed observes in real material [2,6].

4. Discussion

The discrete model proposed here is a new approach for a better understanding of the growth dynamics in microcrystalline silicon. Its relevance is due to its simplicity: it does not rely on physico-chemical details of the growth process, but focuses on more basic dynamical aspects. By considering two key ingredients: (1) incoming particles that take, after deposition, a finite number n of possible states and (2) a threshold value t for the influence of the neighborhood, this model renders the characteristics of the evolution of surface roughness, crystalline fraction and the microstructure of the material as experimentally observed.

Parameter range: The conical shape of the crystalline grains and the presence of the amorphous phase are not critically dependent on the model parameter values n and t . Indeed, for a given number of states n , a low crystalline threshold t promotes crystalline material growth (because less neighbors in the same state are required to set the newly deposited particle to that state). Similarly for a given t , a small number of states n promotes crystalline growth. Therefore, if one increases

n and one simultaneously decreases t (and vice versa), one obtains roughly the same microstructure.

Nucleation and substrate influence: Nucleation happens more often for low values of n and/or t . As no effect of the substrate on the deposited particle state is incorporated in the model, the first mono-layers tend to be amorphous. Additional parameters could, thus, be introduced in order to take into account the possible physico-chemical influence of the substrate on nucleation.

Particle size: For reasons of computational complexity, atomistic level simulations are not possible if one desires to capture the microstructure of the material on the micrometer scale. Thus, within this model, the incoming particle does not represent a radical or a molecule from the plasma phase, but rather a short-range ordered cubic ‘brick’. In our simulations, the brick edge measures one network unit. In Fig. 1(a)), the discretization of the AFM scan of the rough substrate yields a network unit of about 2 nm.

Particle state : The selected particle’s state represents its crystallographic orientation, meaningful only if one considers its position relative to its neighbors. In a real material, a grain boundary is defined as a region over which the crystallographic misorientation α between two grains exceeds several degrees. Depending on this value, polycrystalline material will be reproduced by a finite number of possible crystalline orientations. The latter can be calculated as follows: considering the ratio between the solid angle of the cone Ω with an aperture $\alpha/2$ and the unit sphere surface A , one obtains

$$n = \frac{1}{8} \frac{A}{\Omega} = \frac{1}{4(1 - \cos \frac{\alpha}{2})},$$

where the factor $1/8$ takes into account the symmetries of the cubic lattice. For $\alpha = 24^\circ$, one obtains approximately $n = 12$ states, which corresponds to the value used for the simulations presented in Fig. 1(a)). From this point of view, n corresponds to the possible crystallographic orientations of grains. The experimentally observed conglomerates of crystallites are, thus, reproduced in the model by domains filled with a single color.

The model presented here, does not reproduce, in its simplest version cracks as observed experimentally between the crystalline grains because no shadowing (no particle falls obliquely) and/or lateral sticking of the particles is included in this model. Furthermore, the substructure observed in our TEM micrographs (see Fig. 1(b)) within the crystalline domains is not reproduced. This substructure corresponds to crystalline grains that are less misoriented (e.g. twins).

A possible extension of the model could allow for the presence of ‘defects’ in the crystalline domains (that could correspond e.g. to dangling bonds or to more or

less passivated grain boundaries) by introducing a probability of departing from the first selection rule.

Finally, because the model does not rely on specific physico-chemical interactions on the growing surface, it could indeed apply (may be with modification of the selections rules), to the simulation of growth dynamics of other PECVD grown thin films, such as diamond-like carbon.

5. Conclusions

A 3D dynamical growth model is proposed here; it constitutes a new general approach that allows for a better understanding of the conditions prevailing for various forms of microcrystalline growth. Here, only the essential growth mechanisms (random deposition, local relaxation and desorption) are considered. After random deposition and local relaxation of an incoming particle, one among a finite number n of possible states is selected according to the first selection rule. This rule involves a threshold value t for the influence of the neighborhood. The particle’s state represents its crystallographic orientation relative to its neighbors. Desorption is introduced with a model parameter d that corresponds to the preferential etching of amorphous material, as observed experimentally. With a large set of model parameter values (n , t , d) the main experimental observation about growth of microcrystalline silicon have been reproduced:

- Phase transition versus etching and thickness.
- Conical crystalline grains.
- Crystalline phase evolution versus thickness.
- Roughness evolution versus accumulated film thickness.

The approach described here does not critically depend on any particular assumptions about the nature of the incoming particles and the desorption process. In its simplest form, this model could be used for the study of other materials exhibiting complex microstructures and/or an amorphous/microcrystalline transition, such as diamond like-carbon.

Finally, the model presented here will be extended and improved in order to reproduce cracks and voids as well as sub-grains.

Acknowledgements

The authors thank Professor H. Beck for his support. They acknowledge financial support from the Swiss Office Fédéral de l’Energie (OFEN) under contract No. 36487 as well as from the Swiss National Science Foundation under grant FN66985.

References

- [1] A. Shah, J. Meier, E. Vallat-Sauvain, N. Wyrsh, U. Kroll, C. Droz, U. Graf, *Solar Energ. Mater. Solar Cells* 78 (2003) 469.
- [2] J. Bailat, E. Vallat-Sauvain, L. Feitknecht, C. Droz, A. Shah, *J. Appl. Phys.* 93 (2003) 5727.
- [3] A. Matsuda, *Thin Film Solids* 377 (1999) 1.
- [4] C.C. Tsai, *Amorphous Silicon and Related Materials*, World Scientific, 1988.
- [5] R.W. Collins, A.S. Ferlauto, G.M. Ferreira, C. Chen, K. Joohyun, R.J. Koval, L. Yeeheng, J.M. Pearce, C.R. Wronski, *Solar Energ. Mater. Solar Cells* 78 (2003) 143.
- [6] T. Mates, A. Fejfar, I. Drbohlav, B. Reze, P. Fojtik, K. Luterova, J. Kocka, C. Koch, M.B. Schubert, M. Ito, *J. Non-Cryst. Solids* 299–302 (2002) 767.
- [7] A.L. Barabasi, H.E. Stanley, *Fractal Concepts in Crystal Growth*, Cambridge University, 1995.
- [8] J. Meier, U. Kroll, S. Dubail, S. Golay, S. Faÿ, J. Dubail and A. Shah, in: *Proceedings of the 28th IEEE Photovoltaic Specialists Conference*, Anchorage, AK 2000, p. 746.
- [9] J. Benedict, R. Anderson, S.J. Klepeis, *MRS Symp. Proc.* 254 (1992) 121.